

Dispersion error in white-light Linnik interferometers and its implications for evaluation procedures

Andreas Pförtner and Johannes Schwider

White-light interferometry is a standard optical tool with which to measure profiles of discontinuous structures such as diffractive optical elements. But there is one outstanding technological problem: The interferometers have to be symmetric; i.e., the geometrical path lengths in glass have to be the same for both interferometer arms. If these paths in glass are not equal within the field of view, a dispersion error will occur that is rather complicated to compensate for. The error appears in the measured profile in the form of steps of $\lambda/2$ in height. A simulation of interferograms disturbed by dispersion deviations is presented, and an algorithm is introduced that eliminates the steps without changing the actual phase information or averaging neighboring pixels. The results are shown with simulated and real data.

© 2001 Optical Society of America

OCIS codes: 120.6550, 120.2830, 120.3180, 120.3940, 120.4290, 180.3170.

1. Introduction

White-light interferometry is a powerful tool with which to measure the profiles of discontinuous structures, e.g., diffractive optical elements. Compared with tactile methods, e.g., atomic-force microscopy, this method has some advantages. It is much faster and almost as precise. It is possible to achieve vertical resolutions below 1 nm and lateral resolutions near the diffraction limit.¹⁻⁵

But there is one outstanding technological problem: A dispersion error as a result of a small asymmetry in the interferometer is highly likely. This means that the geometrical path lengths of the light rays in dispersive elements such as glass are different in the two interferometer arms. As an example, we consider the Linnik interferometer (Fig. 1), which provides highest lateral resolution because the imaging system is placed within the interferometer, enabling high numerical apertures to be achieved. Because of the design, it is also the most sensitive type of interferometer to dispersion problems. Possible reasons for deviations from symmetry are that

two microscope objectives may not be identical in their glass paths and, in most cases, that a beam-splitter cube may not be perfectly cubic.⁶ As long as the dispersion deviation does not vary in the field of view there is no problem, in principle. But, if the dispersion deviations depend on the field of view, problems occur in form of so-called ghost steps when the profile of the object under test is evaluated by use of an algorithm that makes use not only of the envelope but also of the phase of the white-light interference patterns. The evaluation of the actual phase is essential if highest vertical resolutions shall be achieved.

In what follows, we present a brief description of the evaluation of white-light interference patterns. Then white-light interferograms that comprise dispersion deviations are simulated and an algorithm is presented that compensates for the errors that arise from the dispersion deviations with real and simulated data.

2. Evaluation of White-Light Interference Patterns

White-light interferometry uses the fact that high-contrast fringes are visible only if the optical path difference between the two interferometer arms is a few micrometers, depending on the bandwidth of the light source used. So if, e.g., a binary diffractive optical element is scanned through the focal plane, a set of white-light interferograms (Fig. 2) for each pixel will be produced that carries the necessary information for reconstruction of the object profile.

For detection of the position of the contrast maxi-

The authors are with the Lehrstuhl für Optik, Universität Erlangen-Nürnberg, Staudtstrasse 7, D-91058 Erlangen, Germany. A. Pförtner's e-mail address is pfoertner@optik.uni-erlangen.de.

Received 31 January 2001; revised manuscript received 18 July 2001.

0003-6935/01/346223-06\$15.00/0

© 2001 Optical Society of America

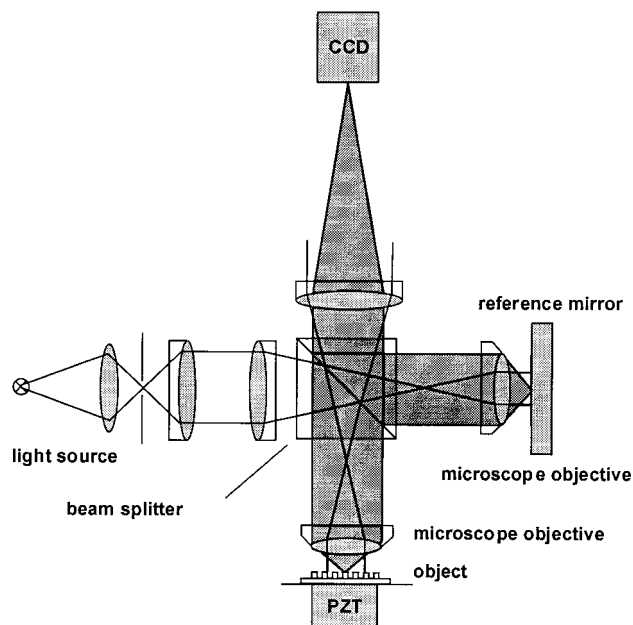


Fig. 1. Schematic of a Linnik interferometer: PZT, piezoelectric transducer; CCD, charge-coupled device.

one can simply use the fact that the Fourier transform, $\text{FT}\{ \}$, of a function $f(z)$ that is shifted on the z axis by z_0 results in terms of the Fourier transform of that function times a phase factor (shift theorem of the Fourier transformation):

$$\text{FT}\{f(z - z_0)\} = \text{FT}\{f(z)\}\exp(-ikz_0), \quad (1)$$

where k is the wave number. If it can be assumed that the function $f(z)$ remains the same for all pixels, the information is contained only in the additional phase Φ that results from the shift z_0 of the Fourier

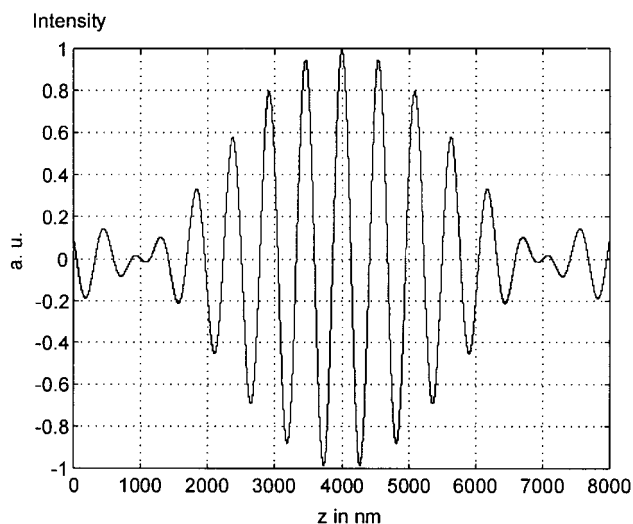


Fig. 2. White-light interferogram seen by a single pixel of a CCD camera during a Z scan (simulated).

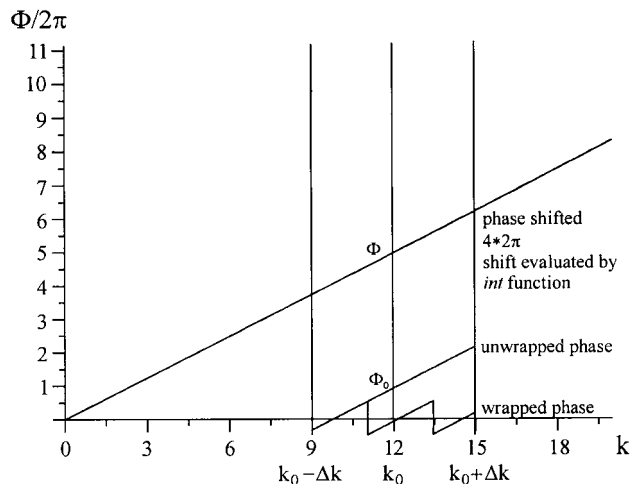


Fig. 3. Procedure for evaluation of z_0 .

transform, which is contained in the exponential function of Eq. (1):

$$\Phi := kz_0. \quad (2)$$

Phase Φ is a linear function in wave number k whose slope is z_0 . In practice, the object is sampled at constant intervals, and one has to take care of the limitations of the sampling theorem. After Fourier transforming an interferogram and evaluating the phase, we obtain a wrapped straight line in k space in the spectral region of the light source. The straight line results from the fact that the phase varies if the wavelength is tuned to a specific constant optical path difference (OPD). In principle, there is no difference between evaluation of the z_0 positions and evaluation of the OPD, e.g., in a dispersive white-light interferometer.⁷ In a next step the wrapped straight line that represents the phase values must be unwrapped. If only low precision is needed, slope z_0 of the straight line in the spectrum can be determined by a linear fit centered about an arbitrary wave number k_0 within the spectrum of the light source. So the position h of the interferogram along the optical axis of the interferometer,

$$h = z_0/2, \quad (3)$$

is also known. The factor 2 in the denominator results from fact that we are using a reflection setup in which the OPDs introduced are doubled. These positions h for every pixel finally represent the measured profile. If high precision is demanded, the situation becomes a bit more involved. The derivation is illustrated in Fig. 3. Now, the phase value Φ_0 at k_0 that results from the fit also must be used for the determination of h . Knowing that the straight line must theoretically cross the point $\Phi(0) = 0$, one can easily determine the vertical shift of the fitted

straight line in steps of 2π such that the condition $\Phi(0) = 0$ is fulfilled. Now one finally has

$$\Phi = \Phi_0 + 2n\pi, \quad n = 0, \pm 1, \pm 2, \pm 3 \dots, \quad (4)$$

$$h = \Phi/2k_0. \quad (5)$$

This procedure results in an algorithm published by de Groot⁸:

$$h = \frac{1}{2k_0} \left[\Phi_0 - 2\pi \operatorname{int} \left(\frac{\Phi_0 - z_0 k_0}{2\pi} \right) \right]. \quad (6)$$

The function int rounds the value in brackets to yield n . This algorithm works even if there is a certain dispersion error, as long as this error remains laterally constant. In that case $\Phi(0) = \varphi$, but offset phase φ can be used for correction. In fact, there is always a specific contribution to φ that is different from zero because of the test object's properties.^{8,9} If φ does not remain laterally constant, either the interferometer has to be calibrated or one has to find an error-checking algorithm. To find such an algorithm, we take a brief look at the theory of white-light interferograms.

3. Simulation of White-Light Interferograms that Comprise Dispersion Deviations

One can simulate white-light interferograms by summing up monochromatic interference patterns of a two-beam interferometer.¹⁰ For all two-beam interference patterns the following equation holds:

$$I[z(x, y)] = I_0 \{1 + V \cos[kz(x, y)]\}. \quad (7)$$

The position of the OPD equal to zero is the same for all wavelengths. Integrating over k results in the following equation, for which, for the sake of simplicity, it has been assumed that intensity I_0 and visibility V are independent of k :

$$\begin{aligned} I_{\text{WL}}[z(x, y)] &= \int_{k_1}^{k_2} I_0 \{1 + V \cos[kz(x, y)]\} dk \\ &= (k_2 - k_1) I_0 \left\{ 1 + V \operatorname{sinc} \left[\frac{k_2 - k_1}{2\pi} \right. \right. \\ &\quad \left. \left. \times z(x, y) \right] \cos \left[\frac{k_2 + k_1}{2} z(x, y) \right] \right\}. \quad (8) \end{aligned}$$

The white-light interferogram is a cosine modulated with the mean wave number with a sinc function as an envelope. A dispersion error that is due to asymmetries in the interferometer will shift the position where $\text{OPD} = 0$ for each wavelength by a small amount. One can simulate this shift by assuming a linear phase shift in k without being too unrealistic. So we add a term $c(k - k_0)$ to the phase of the inter-

ference term, where c is a constant value that controls the dispersion:

$$\begin{aligned} I_{\text{WL}}[z(x, y)] &= \int_{k_1}^{k_2} I_0 \{1 + V \cos[kz(x, y) \\ &\quad + (k - k_0)c(x, y)]\} dk \\ &= (k_2 - k_1) I_0 \left\{ 1 + V \operatorname{sinc} \left[\frac{k_2 - k_1}{2\pi} \right. \right. \\ &\quad \left. \left. \times [z(x, y) + c(x, y)] \right\} \right. \\ &\quad \left. \times \cos \left[\frac{k_2 + k_1}{2} [z(x, y) \right. \right. \right. \\ &\quad \left. \left. \left. + c(x, y)] - k_0 c(x, y) \right] \right\}. \quad (9) \end{aligned}$$

Considering the white-light interferograms obtained, one can conclude that the envelope is obviously moving. The phase of the interferograms is shifted only slightly, depending on k_0 , because the last term in the cosine function of Eq. (9) compensates for the shift introduced by c (Fig. 4). If k_0 is chosen to be the mean wave number, the phase of the interferogram does not move at all compared with that for a calculation without any dispersion deviations. One could add a more appropriate function for the dispersion deviation if one wanted to be more realistic. When the parameter c that controls the dispersion crosses the values

$$c = \frac{(2m + 1)\pi}{k_0} = \frac{(2m + 1)}{2} \lambda_0, \quad m = 0, \pm 1, \pm 2, \dots, \quad (10)$$

i.e., if the maximum of the sinc function coincides with a minimum of the cosine function on the right-hand side of Eq. (9), a critical value for the algorithm [Eq. (5)] is reached. In that case, the factor

$$n := \operatorname{int} \left(\frac{\Phi_0 - z_0 k_0}{2\pi} \right) \quad (11)$$

will lead to a different position of the interference order zero compared with that in the dispersion-free interferogram.

One can physically realize this situation by putting an additional plane glass plate into one interferometer arm with a specific thickness d . In most cases a beam-splitter cube causes this effect because the beam splitter is not perfectly cubic. Calculating the dispersion deviation of an additional glass plate, we found that unwanted steps occur at

$$d = \frac{ck_0}{2k_1 k_2 \gamma} = \frac{(2m + 1)\pi}{2k_1 k_2 \gamma}, \quad \gamma = \frac{n_1 - n_2}{k_1 - k_2}, \quad (12)$$

where n_1 and n_2 are the indices of refraction for wave numbers k_1 and k_2 , respectively, γ is the slope of linear dispersion, and the factor 2 in the denominator

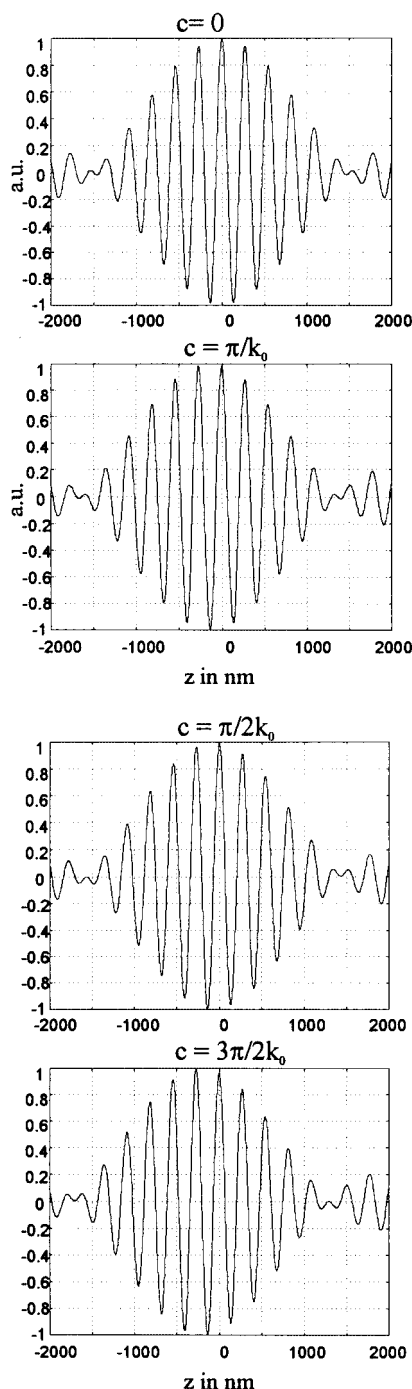


Fig. 4. Shift of the envelope at four values of c (simulated).

results from passing the glass plate twice in a reflection setup.

When the thickness of the glass plate is increased, the first step occurs at a thickness of $3.44\text{ }\mu\text{m}$, and further steps occur every $6.87\text{ }\mu\text{m}$ of a BK7 glass plate, assuming a light source with a constant emissivity of $400\text{--}600\text{ nm}$. If the dispersion deviation changes slightly across the profile as a result of variations of asymmetries in the field, this change has fatal consequences. A ghost step with the height of

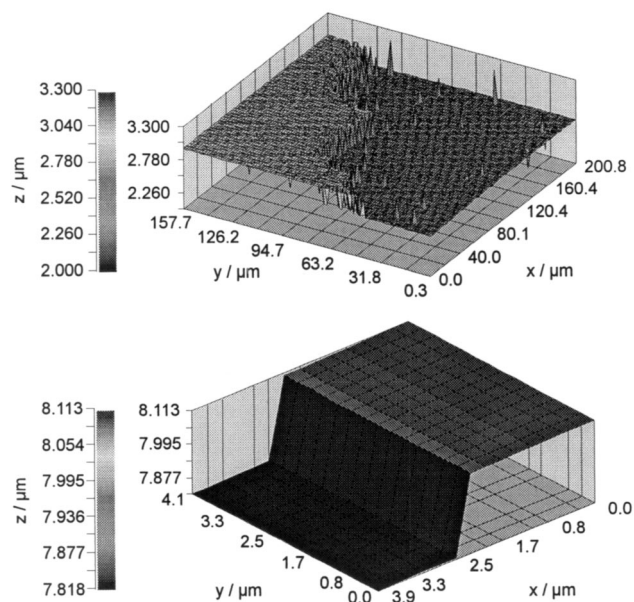


Fig. 5. Profiles that experience a dispersion error (top, real; bottom, simulated).

$\lambda_0/2$ will occur in the measured profile, and the surface will show a small gradient that depends on the value of k_0 . A real surface and a simulated plane surface that suffer from such a dispersion deviation are shown in Fig. 5. Note the tiny slope in the simulated data, which results from choice of a value of k_0 that is different from the mean wave number.

Let us consider the consequences for beam splitter cubes: First, they are not cubic, but this results only in a constant error. Second, the right angles of the prisms are not perfectly 90° . We calculated the maximum allowable deviation from a right angle for one BK7 prism of the beam splitter cube. The other angle was assumed to be perfect. At a beam diameter of $\sim 5\text{ mm}$, the deviation from a right angle may be only $2'22''$. This result is close to or in some cases already less than the maximum tolerance specified by most manufacturers. Furthermore, for a Linnik interferometer we need two identical microscope objectives, which are also difficult to obtain. So we developed a software solution to the dispersion problem.

4. Algorithm for Compensation of the Dispersion Error

De Groot's algorithm uses the phase information of the Fourier transform. It is approximately ten times more sensitive than the result of using only the slope of a straight line fitted to the phase values. As the more-precise algorithm experience ghost steps and the simpler algorithm that uses only the envelope does not, one might conclude that one can easily compensate for the error by simply subtracting the result of the simple algorithm from the result of the precise algorithm to get a correction map for the precise algorithm. But if this is done the following problem occurs: The result shows a saw-tooth-like

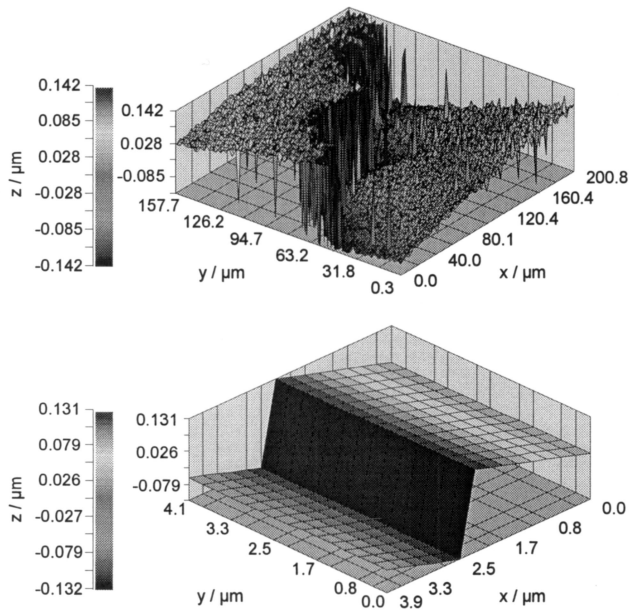


Fig. 6. Result after the results of both algorithms are subtracted from each other (top, real; bottom, simulated).

behavior after the results of the two algorithms are subtracted (Fig. 6).

In that form the data produced do not help much. The shape reminds us of the wrapped phase in phase-shift interferometry. In fact, unwrapping this sawtooth-like map results in an unwrapping map that can be used directly for correction of the dispersion error. To get a fast algorithm we generate a special set of data consisting only of the values 1, 0, and -1:

$$u := 2 \operatorname{int} \left(\frac{\Phi_0 - z_0 k_0}{2\pi} \right) - \operatorname{int} \left(\frac{\Phi_0 - z_0 k_0}{2\pi} + \frac{1}{4} \right) - \operatorname{int} \left(\frac{\Phi_0 - z_0 k_0}{2\pi} - \frac{1}{4} \right). \quad (13)$$

This operation determines whether the envelope has moved relative to a phase close to a critical value. The interval that marks the position of the envelope as critical has a chosen width, $1/4$. Any other value from 0 to $1/2$ is also possible. If the position of the envelope runs across a critical value, a step from 1 to -1 or vice versa will occur. This map can be unwrapped like the wrapped phase in phase-shift interferometry by use of a special algorithm. This algorithm makes use of the fact that the slope of the dispersion error is small. In most cases there are only one or two steps that are widely separated across the field of view. For that reason we decided to use an algorithm that divides the map into regions that contain pixels with the same value. To keep the number of regions small, we still regard pixels that are separated by as many as 3 pixels with the same value as belonging to the same region. The unwrapping of the regions starts with the largest region,

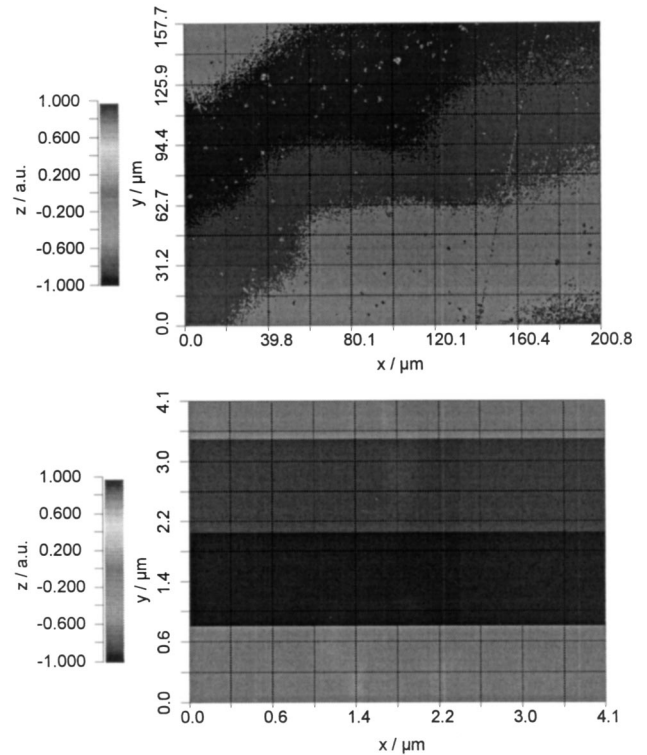


Fig. 7. Map generated for the unwrapping algorithm that contains only the values 1, 0, and -1 (top, real; bottom, simulated).

which is compared with the second largest, and so on. Regions that need to be unwrapped get marked. Again, examples of the maps in which only the values 1, 0, and -1 occur and that have to be unwrapped are shown for real measurement and simulated data (Fig. 7).

This procedure produces an unwrapping map that

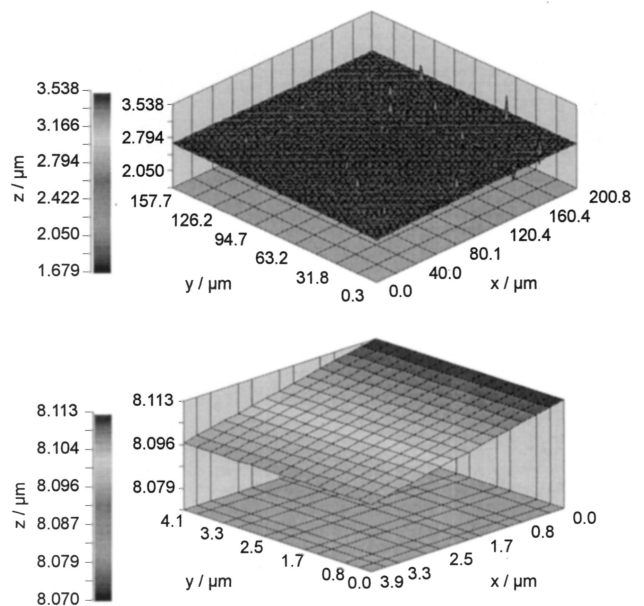


Fig. 8. Corrected profiles (top, real; bottom, simulated).

contains only integers. Finally, the values of that map must be multiplied by $\lambda_0/2$ and added to the original profile evaluated by the de Groot algorithm. The result of correction of the dispersion error after unwrapping is shown in Fig. 8. The ghost steps are eliminated, with no change in the original phase information. There is no averaging of neighboring phase values. One can also determine the small slope in the simulated data, as predicted.

5. Conclusion

The influence of small asymmetries in a white-light interferometer that arise from, e.g., an imperfect beam splitter was considered. It turned out that especially small angular errors of the prisms or of beam-splitter plates cause a shift of the envelope of a white-light interferogram that leads to ghost steps in the measured profile of the object under test. As long as the deviation remains constant in the field of view, this deviation can easily be corrected. But the deviation will cause a severe problem if the error is not constant. To resolve this problem we presented an algorithm that eliminates the ghost steps without

changing the original phase information or averaging neighboring phase values.

References

1. G. S. Kino and S. S. C. Chim, "Mirau correlation microscope," *Appl. Opt.* **29**, 3775–3783 (1990).
2. Th. Dresel, G. Häusler, and H. Venzke, "Three-dimensional sensing of rough surface by coherence radar," *Appl. Opt.* **31**, 919–925 (1992).
3. P. Sandoz and G. Tribillon, "Profilometry by zero-order interference fringe identification," *J. Mod. Opt.* **40**, 1691–1700 (1993).
4. Zygo Corporation, "What is frequency domain analysis," R & D Tech. Bull. PdG 9/93 (Zygo Corp., Middlefield, Conn., 1993).
5. A. Harasaki, J. Schmidt, and J. C. Wyant, "Improved vertical-scanning interferometry," *Appl. Opt.* **39**, 2107–2115 (2000).
6. K. B. Farr and N. George, "Beamsplitter cube for white light interferometry," *Opt. Eng.* **31**, 2191–2196 (1992).
7. J. Schwider and L. Zhou, "Dispersive interferometric profilometer," *Opt. Lett.* **19**, 995–997 (1994).
8. P. de Groot and L. Deck, "Surface profiling by analysis of white-light interferograms in the spatial frequency domain," *J. Mod. Opt.* **42**, 389–401 (1995).
9. A. Harasaki, J. Schmidt, and J. C. Wyant, "Offset of coherent envelope position due to phase change on reflection," *Appl. Opt.* **40**, 2102–2106 (2001).
10. J. Chamberlain, *The Principles of Interferometric Spectroscopy* (Wiley, New York, 1979), pp. 5–11.